*Int. J. Heat Mass Transfer.* Vol. 31, No. 6, pp. 1247–1260, 1988
Printed in Great Britain

0017–9310/88 $3.00 + 0.00


# Natural convection across a vertical layered porous cavity

F. C. LAI
Department of Mechanical Engineering, University of Delaware, Newark, DE 19716, U.S.A.

and

F. A. KULACKI
Department of Mechanical Engineering, Colorado State University, Fort Collins, CO 80523, U.S.A.

(*Received* 18 *May* 1987 *and in final form* 4 *November* 1987)

**Abstract**—Numerical studies are reported for steady-state natural convection in a two-dimensional layered porous cavity heated from the side wall. Emphasis is placed on the effects caused by the sublayer thickness ratio, permeability contrast and non-uniform conductivity in a system comprising two sublayers. Calculations have covered a wide range of these parameters. It has been observed that the flow and temperature fields for a layered structure with $K_1/K_2 < 1$ are completely different from those of $K_1/K_2 > 1$. When the thermal properties are uniform, the average Nusselt number for a layered system of $K_1/K_2 < 1$ is always greater than that of a homogeneous system, and it increases with Rayleigh number, but decreases with the sublayer thickness ratio. For systems of $K_1/K_2 > 1$, the average Nusselt number is always less than that of a homogeneous system, and it increases with both Rayleigh number and the thickness ratio. When there exists a difference in the thermal conductivity of the two sublayers, a second recirculating cell is generated in the less permeable layer for $K_1/K_2 < 1$. The average Nusselt number is found to increase with the conductivity ratio for $K_1/K_2 < 1$, and decrease for $K_1/K_2 > 1$. Heat transfer results including streamline and isotherm patterns, temperature and velocity profiles, and the Nusselt vs Rayleigh number relation in terms of these parameters, are presented.

## INTRODUCTION

OVER THE past years, heat transfer in saturated porous media has received considerable attention because of its important applications in geophysics and energy related engineering problems. These include the utilization of geothermal energy, the control of pollutant spread in groundwater, as well as the design of nuclear reactors, compact heat exchangers, solar power collectors, and high performance insulation for buildings [1, 2]. Heat transfer by natural convection across a porous layer heated from the side is of fundamental importance in many of these applications. The model commonly used consists of a layer with both vertical walls maintained at different temperatures, and with top and bottom walls insulated [3–9]. In fact, in many engineering applications, the temperature of a wall is not uniform but, rather, is a result of the imposition of a constant heat flux. Results for this situation have been reported only in refs. [10, 11]. However, these studies only considered a homogeneous layer, whereas a composite layer, which has also been used widely in engineering practices, has not been studied before.

A review of the literature shows that most previous studies on heat transfer in layered porous media deal only with the horizontal case [13–18]. To our knowledge, only Poulikakos and Bejan [19] have presented a study on vertical layered systems. However, they only studied a system of three sublayers subjected to an end-to-end temperature difference, for a special case of $\alpha_1 = \alpha_3$ and $K_1 = K_3$. Since their interest was on the investigation of channelling effects, the permeability contract they considered was, thus, limited to 0.2 and 5. For permeability ratios $K_1/K_2 \geqslant 10$ and $K_1/K_2 \leqslant 0.1$, heat transfer results have not been reported. In addition, most previous studies on layered porous media have their analyses based on the assumption of uniform thermophysical properties. The differences in the thermal conductivity between sublayers have not been considered before. Therefore, our emphasis in the present study has been placed on a fundamental examination of the effects caused by the sublayer thickness, permeability contrast and non-uniform thermal conductivity.

## FORMULATION AND NUMERICAL METHOD

The geometry considered is a two-dimensional, two-layer porous system (Fig. 1). For each sublayer, it is assumed to be fully saturated and has a different permeability, conductivity and thickness. A constant heat flux is applied to one vertical wall, while the other vertical wall is maintained at a constant temperature $T_c$. The top and bottom surfaces are insulated.

The governing equations based on Darcy's law are given by

## NOMENCLATURE

| | |
|---|---|
| $A$ | aspect ratio |
| $c$ | specific heat of fluid at constant pressure |
| $g$ | acceleration of gravity |
| $\bar{h}$ | average heat transfer coefficient on the heated wall |
| $H$ | height of the porous layer |
| $k$ | effective thermal conductivity of the saturated porous medium |
| $K$ | permeability of saturated porous medium |
| $L$ | width of the porous layer |
| $Nu$ | average Nusselt number, $\bar{h}H/k$ |
| $q$ | constant heat flux |
| $Ra$ | Rayleigh number, $Kg\beta qH^2/\nu\alpha k$ |
| $T$ | temperature |
| $T_c$ | temperature at the cooled wall |
| $u$ | velocity in $x$-direction, $-\partial\psi/\partial y$ |
| $U$ | dimensionless velocity in $x$-direction |
| $v$ | velocity in $y$-direction, $\partial\psi/\partial x$ |
| $V$ | dimensionless velocity in $y$-direction |
| $x, y$ | Cartesian coordinates |
| $X$ | dimensionless distance on $x$-axis, $x/L$ |
| $Y$ | dimensionless distance on $y$-axis, $y/H$. |

Greek symbols

| | |
|---|---|
| $\alpha$ | thermal diffusivity of porous medium, $k/(\rho c)_f$ |
| $\beta$ | thermal expansion coefficient of fluid |
| $\theta$ | dimensionless temperature, $T-T_c/(qH/k_1)$ |
| $\rho$ | density of fluid |
| $\psi$ | dimensional stream function |
| $\Psi$ | dimensionless stream function, $\psi/\alpha$. |

$$\frac{\partial u_i}{\partial x}+\frac{\partial v_i}{\partial y}=0 \tag{1}$$

$$u_i=-\frac{K_i}{\mu}\frac{\partial P_i}{\partial x} \tag{2}$$

$$v_i=-\frac{K_i}{\mu}\left(\frac{\partial P_i}{\partial y}+\rho_i g\right) \tag{3}$$

$$u_i\frac{\partial T_i}{\partial x}+v_i\frac{\partial T_i}{\partial y}=\alpha_i\left(\frac{\partial^2 T_i}{\partial x^2}+\frac{\partial^2 T_i}{\partial y^2}\right) \tag{4}$$

with the subscript $i=1,2$ denoting the sublayers. The corresponding boundary conditions are

$$k_1\frac{\partial T_1}{\partial x}=-q, \quad x=0 \tag{5}$$

$$T_2=T_c, \quad x=L \tag{6}$$

$$\frac{\partial T_i}{\partial y}=0, \quad y=0,H \tag{7}$$

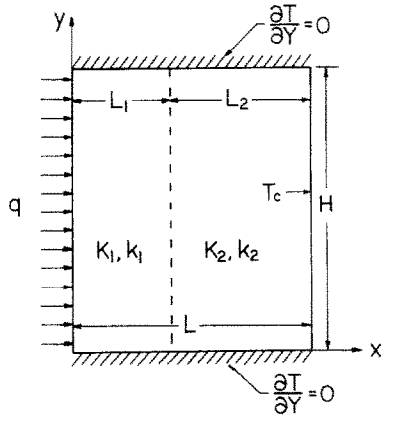


FIG. 1. A two-dimensional, two-layer porous cavity heated with a constant heat flux from the side wall.

$$v_i=0, \quad y=0,H \tag{8}$$

$$u_i=0, \quad x=0,L. \tag{9}$$

At the interface, the appropriate conditions are the continuity of pressure, temperature, horizontal flow and heat flux

$$P_1=P_2 \tag{10}$$

$$T_1=T_2 \tag{11}$$

$$U_1=U_2 \tag{12}$$

$$k_1\frac{\partial T_1}{\partial x}=k_2\frac{\partial T_2}{\partial x}. \tag{13}$$

The justification of these boundary conditions is given by Rana *et al.* [17], and McKibbin and co-workers [13–15].

When the Boussinesq approximation is invoked, the governing equations and boundary conditions can be non-dimensionalized as follows:

$$\frac{\partial^2\Psi_i}{\partial X^2}+A^2\frac{\partial^2\Psi_i}{\partial Y^2}=-Ra_i A\frac{\partial T_i}{\partial X} \tag{14}$$

$$A\left(\frac{\partial\Psi_i}{\partial Y}\frac{\partial\theta_i}{\partial X}-\frac{\partial\Psi_i}{\partial X}\frac{\partial\theta_i}{\partial Y}\right)=\frac{\partial^2\theta_i}{\partial X^2}+A^2\frac{\partial^2\theta_i}{\partial Y^2} \tag{15}$$

where

$$Ra_i=K_i g\beta qH^2/\nu\alpha_i k_1, \quad A=L/H$$

with

$$\frac{\partial\theta_1}{\partial X}=-A, \quad X=0 \tag{16}$$

$$\theta_2=0, \quad X=1 \tag{17}$$

$$\frac{\partial\theta_i}{\partial Y}=0, \quad Y=0,1 \tag{18}$$

$$\Psi_i = 0, \quad Y = 0, 1 \tag{19}$$

$$\Psi_i = 0, \quad X = 0, 1. \tag{20}$$

At the interface, $X = L_1/L$

$$\frac{\partial \Psi_1}{\partial X} = \frac{K_1}{K_2}\frac{\alpha_2}{\alpha_1}\frac{\partial \Psi_2}{\partial X} \tag{21}$$

$$\theta_1 = \theta_2 \tag{22}$$

$$\Psi_1 = \frac{\alpha_2}{\alpha_1}\Psi_2 \tag{23}$$

$$\frac{\partial \theta_1}{\partial X} = \frac{\alpha_2}{\alpha_1}\frac{\partial \theta_2}{\partial X}. \tag{24}$$

In view of the parameters and the complexity involved in this problem, we restrict the present study to the case of $A = 1$, and place our attention to the effects caused by the permeability contrast, $K_1/K_2$, the conductivity difference, $k_1/k_2$ $(= \alpha_1/\alpha_2)$, and the sublayer thickness ratio, $L_1/L$. Since $Ra_1$ is a convenient parameter to use in the analysis, we will call it the 'base' Rayleigh number. The relation between the base Rayleigh number $Ra_1$ and the Rayleigh number of the second layer $Ra_2$ is given by

$$Ra_2 = Ra_1 \frac{K_2}{K_1}\frac{\alpha_1}{\alpha_2}. \tag{25}$$

The dimensionless governing equations (14) and (15) are discretized using the control volume approach described by Patankar [20]. An iterative scheme with under-/over-relaxation parameters is also incorporated to achieve fast convergence. The convective terms in the energy equation have been approximated by upwind differences. This solution procedure has been discussed and successfully used in the study of natural convection in porous media in refs. [11, 12].

The effect of grid fineness on the heat transfer prediction is shown in Fig. 2. As the grids change from $41 \times 41$ to $51 \times 51$, the change in overall Nusselt number is within 2%. For the flow prediction, this effect is similar to that on heat transfer, the maximum stream function changes only by 0.7% as the grids become finer. Therefore, uniform grids, $41 \times 41$, have been used in the present study for better accuracy and less computational cost. A variation of $10^{-4}$ or less in both $\theta$ and $\Psi$ at all nodes in the calculation domain is the convergence criterion for the computation. The conditions at the interface have been implemented in the same way as described by Rana [16]. By using the imaginary nodal points (Fig. 3), equations (21) and (24) can be discretized as

$$\Psi^1_{N,j} = \frac{1}{4}\left[\Psi^1_{N,j-1} + \Psi^1_{N,j+1} + \left(\frac{2K_2/K_1}{1+K_2/K_1}\right)\Psi^1_{N-1,j} + \left(\frac{2\alpha_2/\alpha_1}{1+K_2/K_1}\right)\Psi^2_{N+1,j} + \left(\frac{K_2/K_1}{1+K_2/K_1}\right)Ra_1 + \left(\frac{\alpha_2/\alpha_1}{1+K_2/K_1}\right)Ra_2\right] \tag{26}$$

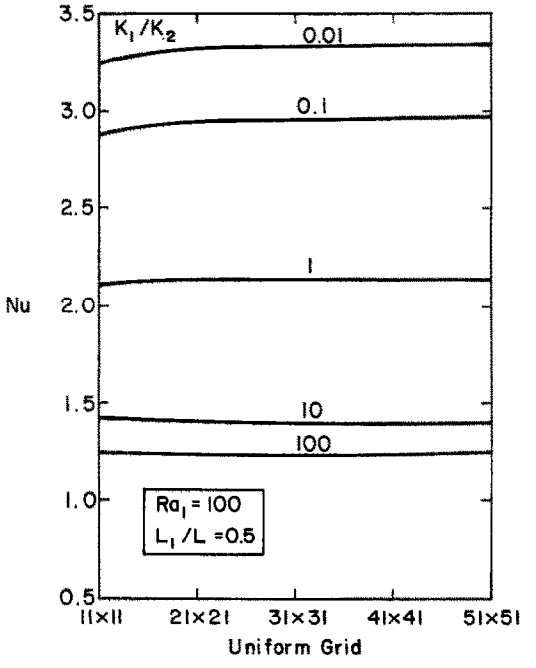


FIG. 2. Effects of grid refinement on average Nusselt numbers.

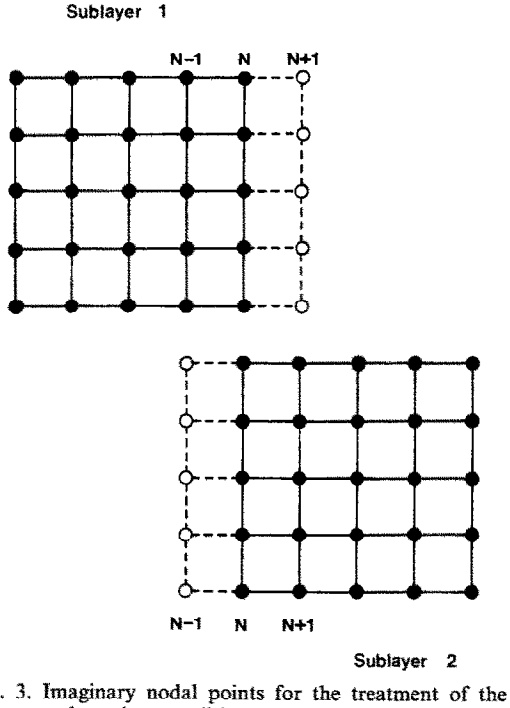


FIG. 3. Imaginary nodal points for the treatment of the boundary conditions at the interface.

$$\theta^1_{N,j} = \frac{4[\theta^2_{N+1,j} + (\alpha_1/\alpha_2)\theta^1_{N-1,j}] - [\theta^2_{N+2,j} + (\alpha_1/\alpha_2)\theta^1_{N-2,j}]}{3[1 + (\alpha_1/\alpha_2)]} \tag{27}$$

As an indication of the proper formulation of the

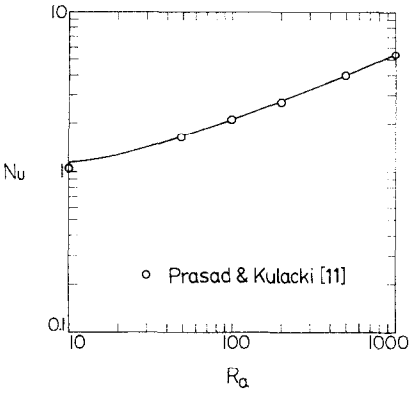


FIG. 4. A comparison of the results obtained from the layered model and homogeneous model.

problem, it has been tested against the corresponding homogeneous case [11], by setting $K_1/K_2$ and $\alpha_1/\alpha_2$ to unity. The results show excellent agreement with each other (Fig. 4), the differences between these two results are within 2.5%.

Calculations have covered a wide range of sublayer thickness ratios, $L_1/L = 0.25$, 0.5 and 0.75, permeability ratios, $0.01 < K_1/K_2 < 100$, and conductivity ratios, $k_1/k_2 = 0.2$ and 0.5. For each layered structure, calculations were performed to obtain results for base Rayleigh numbers up to 1000. It is found that, for a higher base Rayleigh number, convergence is more difficult to obtain for cases where $K_1/K_2 < 1$ than those for $K_1/K_2 > 1$. However, this difficulty can be overcome by using under-relaxation of temperature.

## RESULTS AND DISCUSSION

In this section, the effects of permeability contrast, sublayer thickness ratio and non-uniform conductivity on the temperature and flow fields will be discussed separately. The results of these effects on a system with uniform thermal properties are presented first. Results with a focus on the effect of non-uniform conductivity will then follow.

*Effect of permeability contrast*

The effect of permeability contrast can be clearly seen in Figs. 5 and 6, from which the conductive and convective modes of heat transfer in the sublayers can be easily identified. For a small base Rayleigh number, convection starts in the layer with higher permeability, with the layer of lower permeability remaining in the conductive mode. With an increase in the base Rayleigh number, convective flow begins to penetrate the less permeable sublayer. Eventually, both sublayers are all in the convective mode.

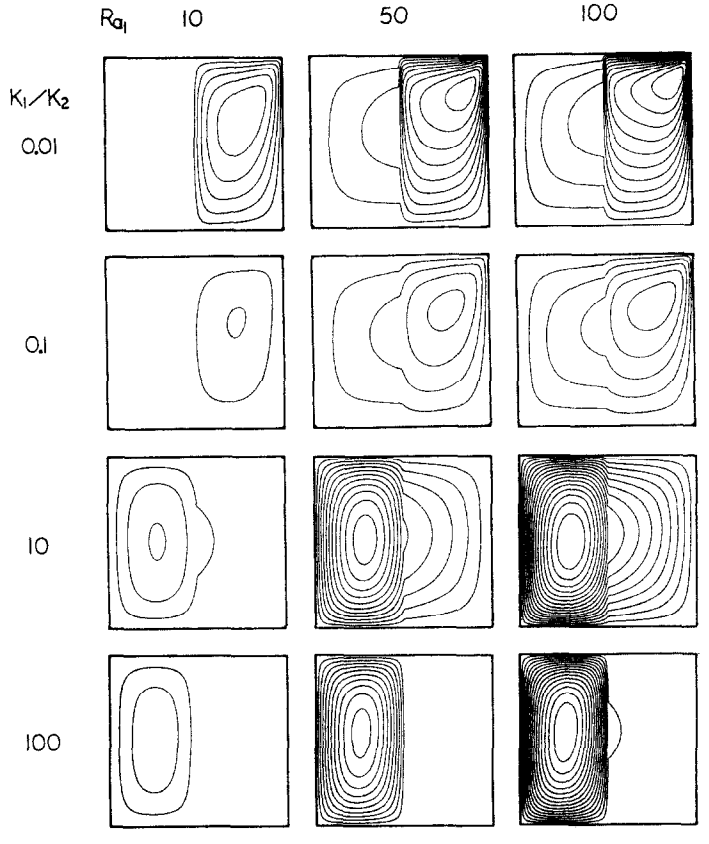


FIG. 5. Effects of permeability contrast: streamline patterns for $L_1/L = 0.5$ ($\Delta\Psi = 1$ for $K_1/K_2 = 0.01$ and 0.1; $\Delta\Psi = 0.1$ for $K_1/K_2 = 10$ and 100).

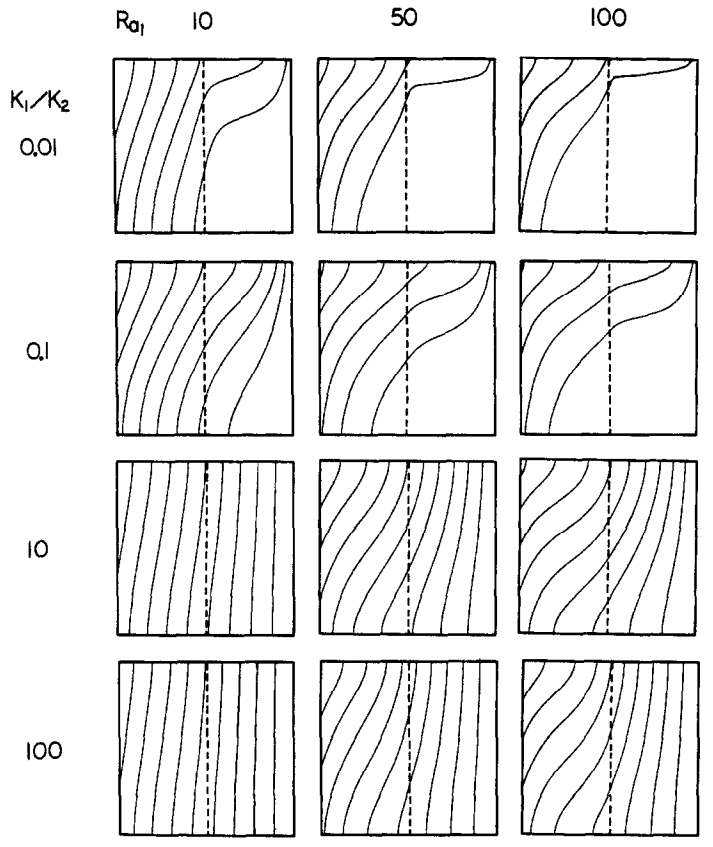


FIG. 6. Effects of permeability contrast: isotherm patterns for $L_1/L = 0.5$.

The interaction between the two heat transfer mechanisms, conduction and convection, can also be easily identified from Fig. 7 which shows the dimensionless temperature distribution across the layers at $Y = 0.5$. By noting the slopes of the temperature distribution, i.e. $\partial\theta/\partial X$, one finds that they are constant in the less permeable sublayer when base Rayleigh number is small, showing that heat is transferred mainly by conduction. With an increase of the base Rayleigh number, the gradual changing of these slopes from a linear variation indicates the initiation of convection.

The strength of the convective flow is shown in Fig. 8. When the base Rayleigh number is small, the first sublayer is effectively in the conduction mode (Fig. 7(a)); therefore, flow moving across the interface is very limited (Fig. 8(a)). As the base Rayleigh number increases, convection is initiated (Figs. 7(b) and (c)) which results in more fluid moving across the interface (Figs. 8(b) and (c)). However, it should be noted that the mass change by convective flow across the interface is minimal for $K_1/K_2 = 100$. For a layered structure of $K_1/K_2 < 1$, the convective flow is almost completely confined to the first layer.

*Effect of sublayer thickness*

For a fixed base Rayleigh number, it is observed that the strength of circulation in the convective cell increases with the thickness ratio $L_1/L$ for $K_1/K_2 > 1$, and decreases for $K_1/K_2 < 1$ (Figs. 9 and 10). For $K_1/K_2 < 1$, a smaller thickness ratio leads to a smaller temperature gradient across the first layer and a higher gradient for the second layer (Fig. 11(a)). This consequently initiates a stronger convective cell in the second layer. With an increase of the thickness ratio, the temperature gradient across the first layer increases, while it decreases in the second layer (Figs. 11(b) and (c)). Because of the permeability contrast, the result of this change is a slight increase in the strength of the convective cell in the first layer, but a significant reduction in the second layer. For $K_1/K_2 > 1$, the situation is just reversed to what has been described for $K_1/K_2 < 1$.

The effect of sublayer thickness on the flow field can be examined from Fig. 12 which shows the vertical velocity across the layers at $Y = 0.5$. The discontinuity of the vertical velocity is due to Darcy's formulation which permits a velocity slip at the interface. As the thickness ratio increases, it is clearly observed that for $K_1/K_2 < 1$, the strength of the convective flow in the first layer only increases slightly, but it decreases considerably in the second layer. The situation is reversed for $K_1/K_2 > 1$. This observation validates the statements we made earlier.

*Effect of non-uniform conductivity*

When there exists a difference in the thermal conductivity of the two sublayers, the temperature and

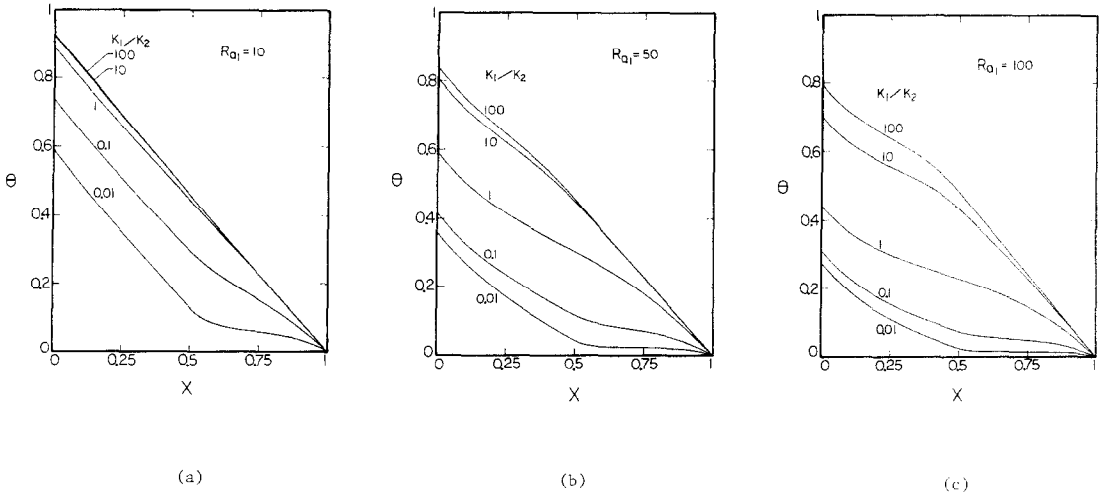


FIG. 7. Effects of permeability contrast: non-dimensional temperature profile across the porous layer at $Y = 0.5$, for $L_1/L = 0.5$.

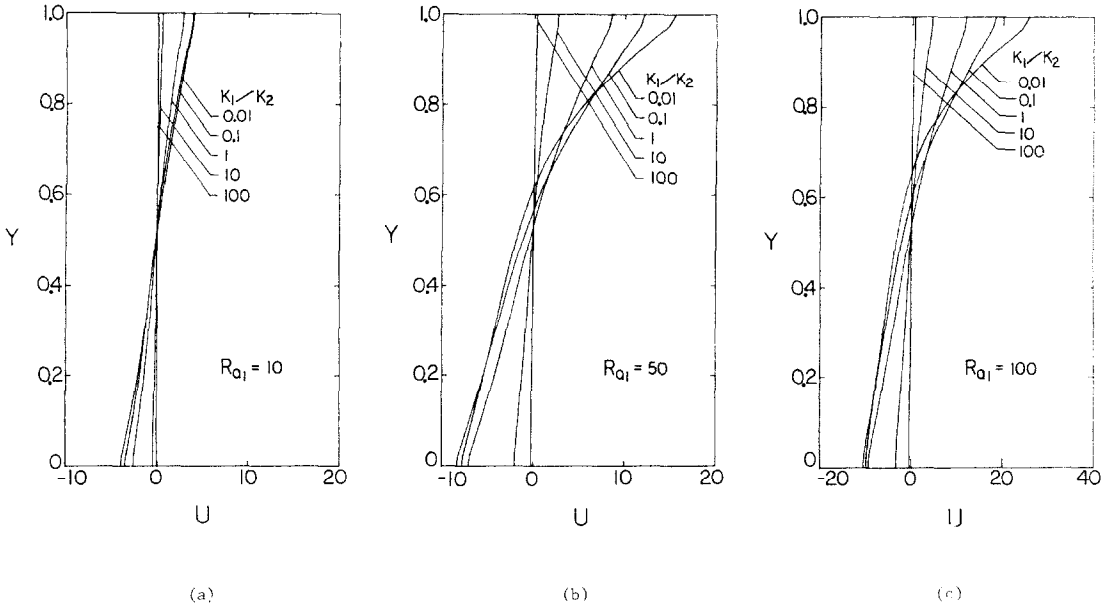


FIG. 8. Effects of permeability contrast: non-dimensional horizontal velocity profiles along the layer interface, for $L_1/L = 0.5$.

flow fields are changed dramatically (Figs. 13 and 14). First, it is noticed that a second recirculating cell is formed in the less permeable layer for systems of $K_1/K_2 < 1$. Second, the strength of the convective cell in a system of $K_1/K_2 > 1$ is increased considerably. The reason for these changes is given as follows: when the first sublayer is less conductive, i.e. $k_1/k_2 < 1$, the temperature gradient across this layer will be higher than it should be if the conductivity were uniform (Fig. 15). It is this elevated temperature gradient that initiates the second recirculating cell for systems of $K_1/K_2 < 1$, and increases the strength of the convective cell for systems of $K_1/K_2 > 1$.

As conductivity becomes more uniform, i.e. $k_1/k_2 \to 1$, the temperature gradient across the first layer then becomes smaller, which in turn leads to a weaker second cell for $K_1/K_2 < 1$ and a convective cell of reducing strength for $K_1/K_2 > 1$. For systems of $K_1/K_2 < 1$, the two recirculating cells will eventually combine into one cell when conductivity becomes uniform.

The effect of non-uniform conductivity on the flow field can be examined through Fig. 16, which shows the horizontal velocity across the interface. As noticed, when the conductivity ratio is small, the flow moving across the interface is very limited as if there were a partition placed in the interface. This is an interesting phenomenon which has not been reported before. As conductivity becomes more uniform, more fluid moves across the interface.

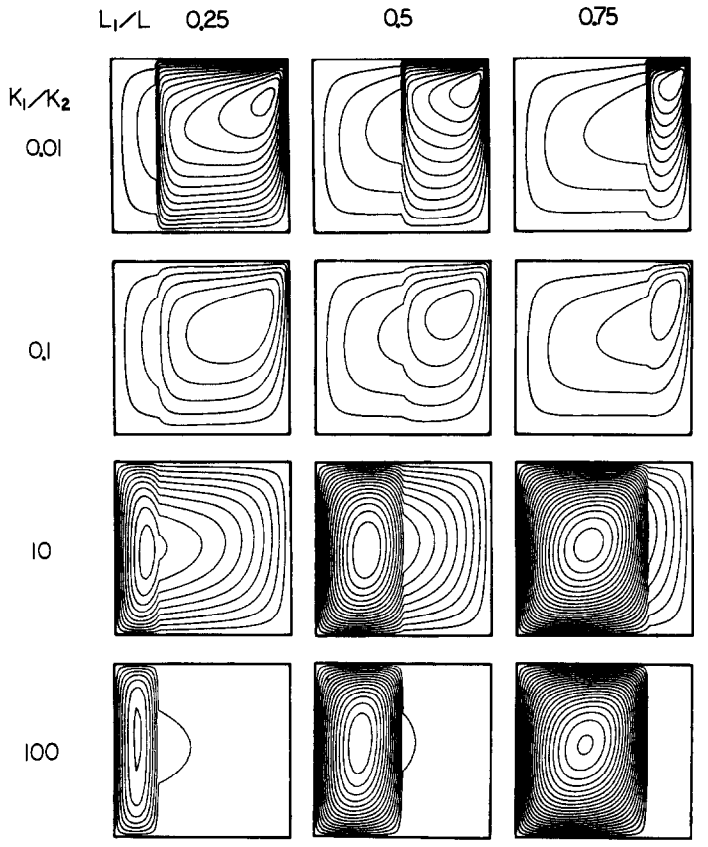


FIG. 9. Effects of thickness ratio: streamline patterns for $Ra_1 = 100$ ($\Delta\Psi = 1$ for $K_1/K_2 = 0.01$ and 0.1; $\Delta\Psi = 0.1$ for $K_1/K_2 = 10$ and 100).

Based on the average temperature of the heated wall

$$\theta_m = \int_0^1 \theta(0, Y)\,dY \tag{28}$$

the mean Nusselt number can be defined as

$$Nu = \frac{1}{\theta_m}. \tag{29}$$

The average Nusselt number is important for design purposes because it gives directly the value of the average temperature for any applied heat flux. It is observed that the ratio of the maximum temperature to the average temperature never exceeds 2, which also has been reported in ref. [11] for a uniform medium.

The effects of permeability contrast, sublayer thickness ratio and non-uniform conductivity on heat transfer results are presented in Figs. 17 and 18. When conductivity is uniform, for systems of $K_1/K_2 < 1$, it is found that the average Nusselt number is always greater than that for a homogeneous layer, and it increases with base Rayleigh number, but decreases with the sublayer thickness ratio. As explained earlier, for $K_1/K_2 < 1$, the temperature gradient across the first sublayer is directly proportional to its thickness. Therefore, an increase of the thickness ratio will only increase the surface temperature of the heated wall (Fig. 11), thus resulting in a decrease of the average Nusselt number.

For systems of $K_1/K_2 > 1$, the average Nusselt number is always less than that of a homogeneous layer, and it increases with both base Rayleigh number and the thickness ratio. As explained earlier also, for $K_1/K_2 > 1$, an increase of the thickness ratio will induce a stronger convective cell in the first layer (Fig. 12), which effectively decreases the surface temperature of the heated wall (Fig. 11). This in turn enhances the average Nusselt number.

It is easy to understand why for systems of $K_1/K_2 < 1$, the average Nusselt number is always greater than that of a homogeneous layer, and is less for systems of $K_1/K_2 > 1$. Imagine a homogeneous system which has a permeability of $K_1$, if part of it (i.e the second sublayer) was replaced by a medium having a higher permeability, the convective cell in this new system will be evidently stronger than that of the original system, which thus increases the average Nusselt number. On the other hand, if the system was partially replaced by a medium of lower permeability, the resulting convective cell will be weaker because of the confinement. This then leads to a decrease of the average Nusselt number.

For systems having non-uniform conductivity, it is

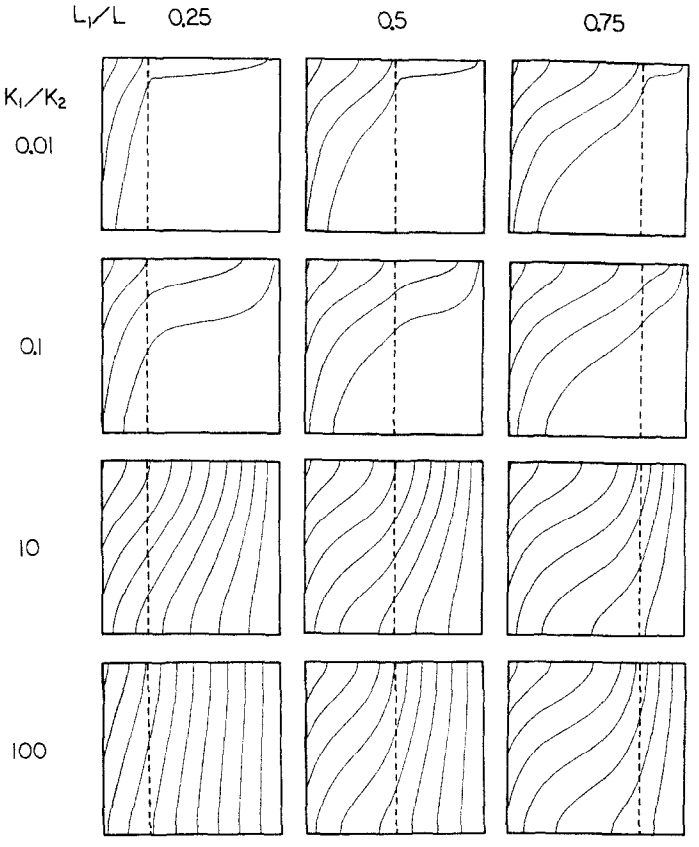


FIG. 10. Effects of thickness ratio: isotherm patterns for $Ra_1 = 100$.

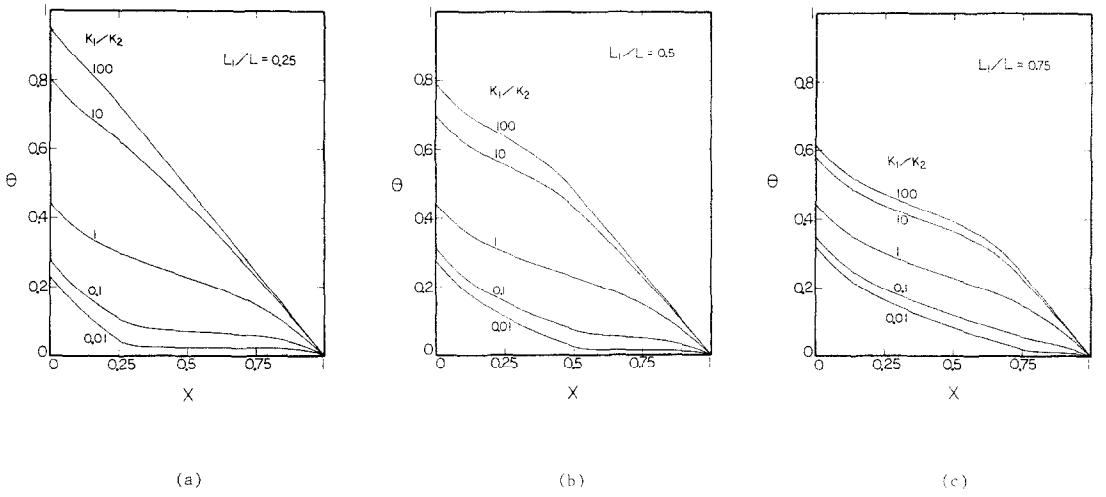


(a) (b) (c)

FIG. 11. Effects of thickness ratio: non-dimensional temperature profile across the porous layer at $Y = 0.5$, for $Ra_1 = 100$.

found that the average Nusselt number increases with the conductivity ratio for $K_1/K_2 < 1$, and decreases for $K_1/K_2 > 1$. As discussed before, the effect of non-uniform conductivity on a system of $K_1/K_2 > 1$ is to increase the strength of the convective cell in the first layer (Fig. 13), which in turn effectively lowers the average temperature of the heated wall (Fig. 15) and, therefore, increases the average Nusselt number.

For systems of $K_1/K_2 < 1$, although a second recirculating cell is generated because of the non-uniform thermal property, its strength is considerably small when compared to that of a system with uniform conductivity (Fig. 13). The average surface temperature thus increases with a reduction of the conductivity ratio (Fig. 15). A direct consequence of this result is a decrease in the average Nusselt number.

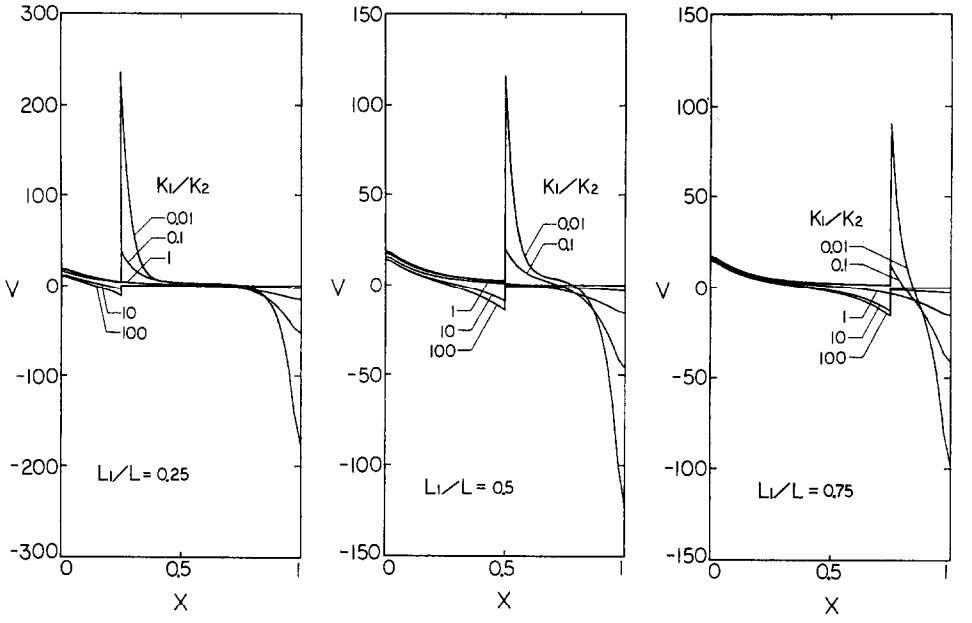


FIG. 12. Effects of thickness ratio: non-dimensional vertical velocity profiles across the porous layer at $Y = 0.5$, for $Ra_1 = 100$.

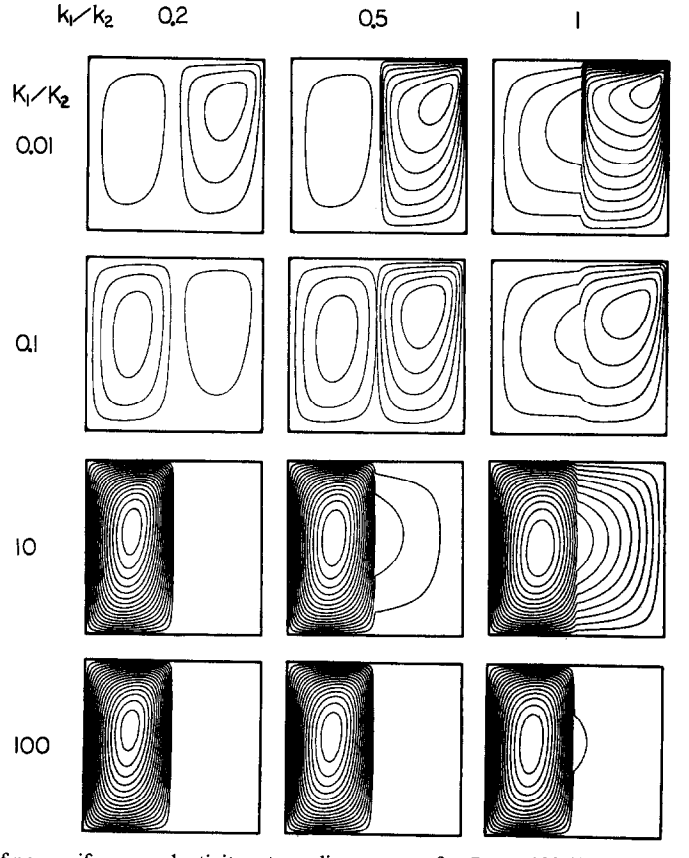


FIG. 13. Effects of non-uniform conductivity: streamline patterns for $Ra_1 = 100$ ($\Delta\Psi = 1$ for $K_1/K_2 = 0.01$ and 0.1; $\Delta\Psi = 0.1$ for $K_1/K_2 = 10$ and 100).

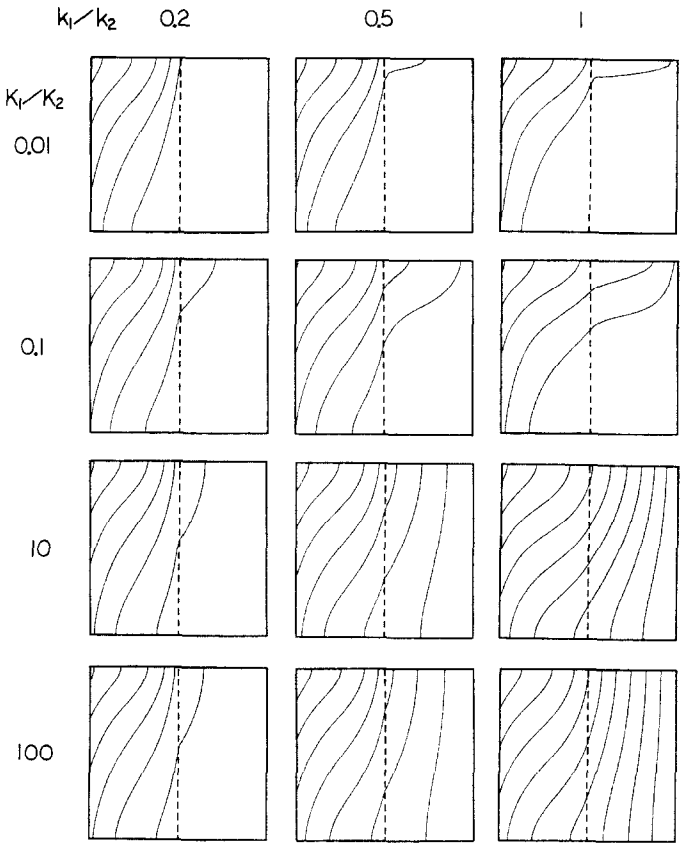


FIG. 14. Effects of non-uniform conductivity: isotherm patterns for $Ra_1 = 100$.

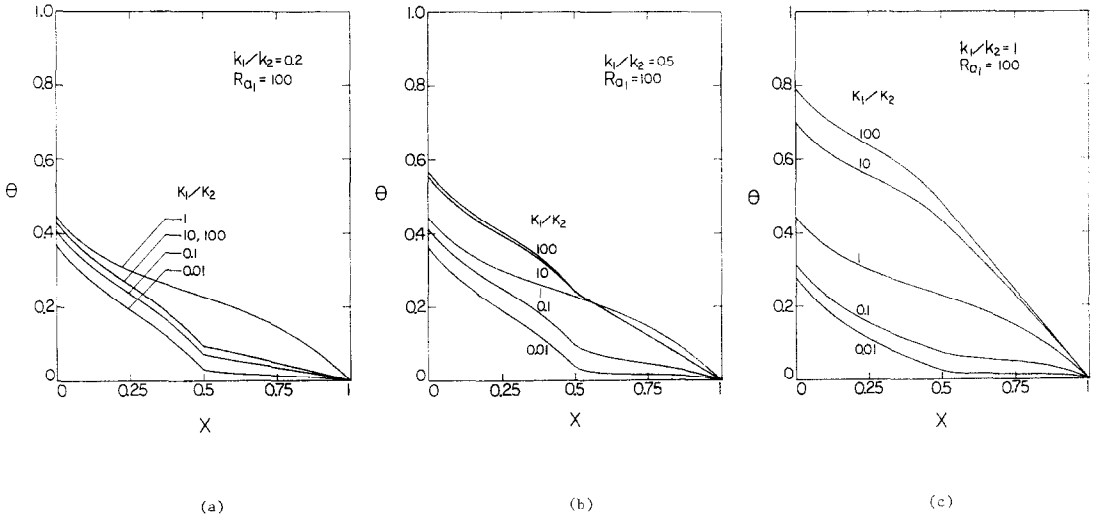


FIG. 15. Effects of non-uniform conductivity: non-dimensional temperature profile across the porous layer at $Y = 0.5$, for $L_1/L = 0.5$ and $Ra_1 = 100$.

## CONCLUSIONS

Steady-state natural convection in a two-dimensional, two-layer vertical porous cavity has been numerically studied for various permeability ratios, sublayer thickness ratios and conductivity ratios. It is found that heat transfer always begins as conduction in the less permeable sublayer, and as convection in the layer with higher permeability. With an increase of the base Rayleigh number, convection in the layer of higher permeability begins to penetrate the less permeable one, and eventually both layers are in the convective mode at sufficiently large $Ra_1$. When there is no conductivity contrast in the system, the average

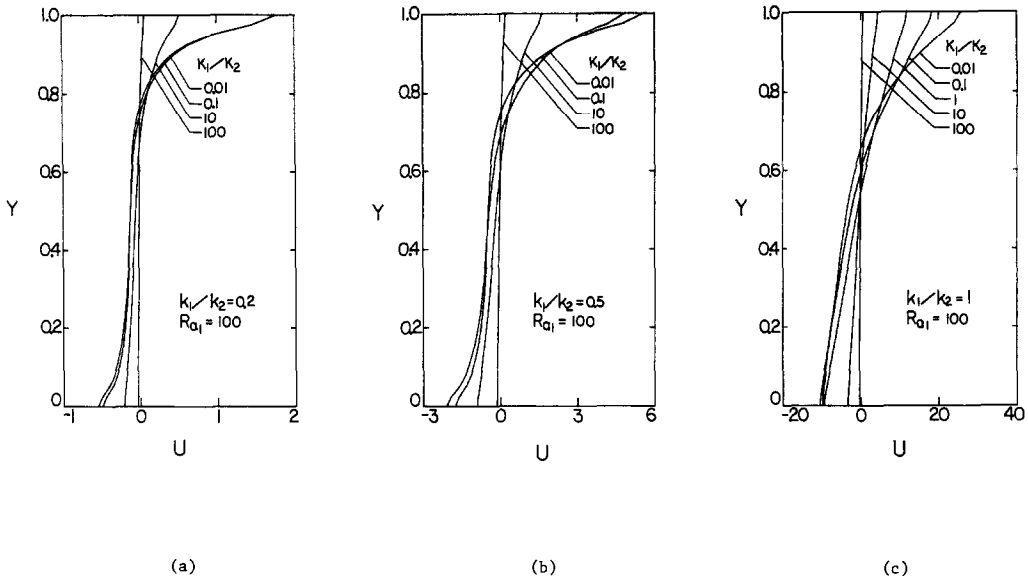


FIG. 16. Effects of non-uniform conductivity: non-dimensional horizontal velocity profile along the interface, for $L_1/L = 0.5$ and $Ra_1 = 100$.

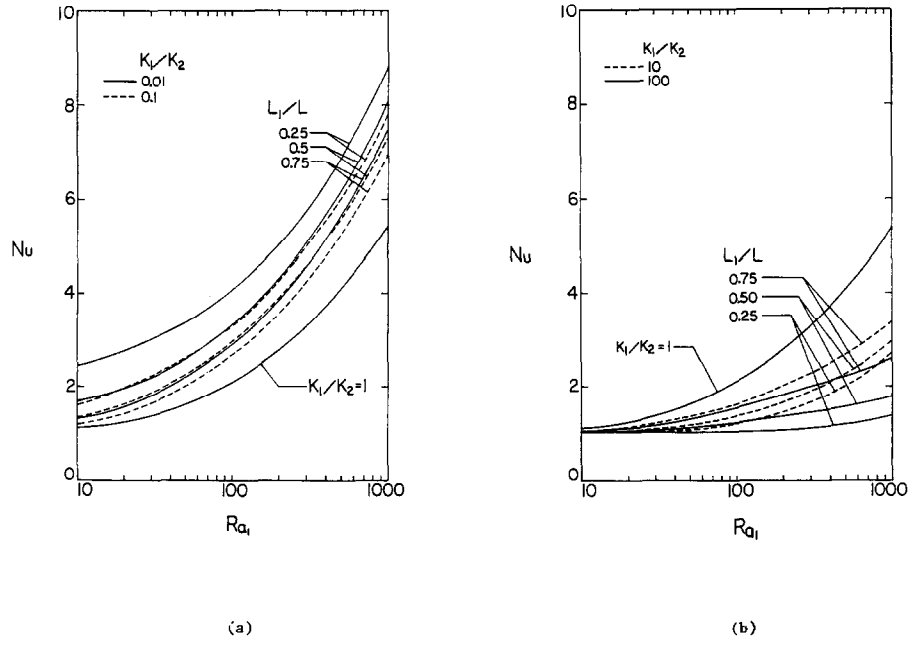


FIG. 17. The effects of permeability contrast and sublayer thickness ratio on the heat transfer results: (a) for $K_1/K_2 = 0.01$ and 0.1; (b) for $K_1/K_2 = 10$ and 100.

Nusselt number for $K_1/K_2 > 1$ is always less than that of a homogeneous medium but is greater for $K_1/K_2 < 1$. For a given $Ra$ the Nusselt number increases with the sublayer thickness ratio for $K_1/K_2 > 1$; but decreases for $K_1/K_2 < 1$. When conductivity is not uniform, the average Nusselt number is found to increase with the conductivity ratio for $K_1/K_2 < 1$, and decrease for $K_1/K_2 > 1$.

While the present study has explored a fundamental problem in a layered porous medium as an extension of several earlier studies, the results have some interesting implications for the important applications like insulation engineering and deep geological disposal of high level nuclear waste. For the former case, as pointed out by Bejan and Anderson [21], the heat loss through a vertical porous layer can be reduced if the convective loop is slender, one way to increase the slenderness of the convection pattern is to insert one

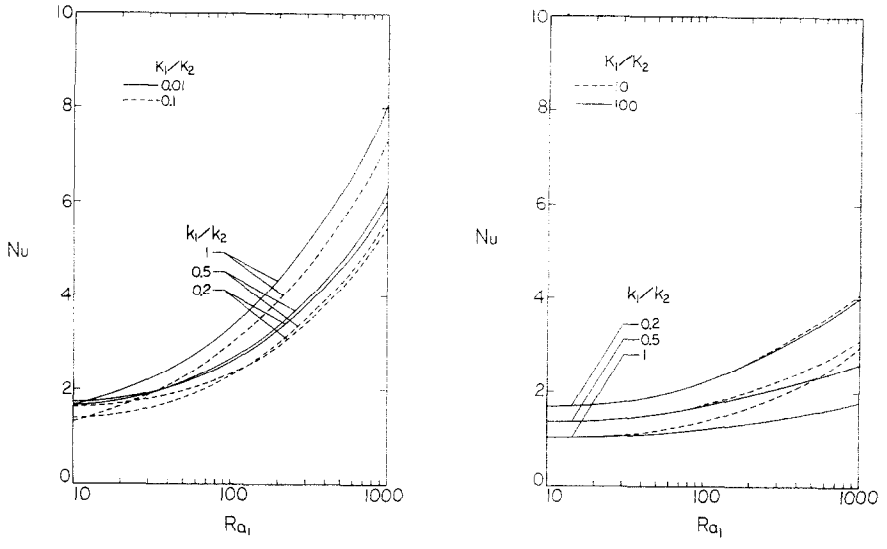


FIG. 18. The effects of non-uniform conductivity on the heat transfer results, for $L_1/L = 0.5$: (a) $K_1/K_2 = 0.01$ and 0.1; (b) $K_1/K_2 = 10$ and 100.

or more vertical partitions in the porous layer. Obviously, another way to achieve this goal is shown in this study by using multiple layers of insulation. With the proper choice of materials, by considering the properties of permeability and conductivity, the layered porous wall can be as effective as the one with vertical partitions, if not better.

For the latter application, the thermally disturbed zone surrounding a repository will generally encompass at least two geologic strata with permeability contrasts possibly as large as 1000, i.e. $1 < K_1/K_2 < 1000$. Such a permeability contrast can result from a combination of fracturing in crystalline rock due to thermal stresses and mining of the repository. Based on the results of our study, the following regional thermal impacts of the repository might be expected.

(1) Penetration of convection into the second sublayer will be minimal, and the second sublayer (even though saturated) will effectively be a conductive barrier.

(2) The average Nusselt number at the heated wall will be smaller than that for a fully convecting, single layer system with a homogeneous permeability. This implies that mean waste package temperatures will be higher and chemical and mass transfer effects near the repository will take on added importance in the containment of radioactivity.

(3) The region of increased permeability around the repository will have a finite horizontal extent as well as a vertical extent. From our earlier study [18], it is known that thermal pluming above the repository will not occur, and the convective component of the radionuclide transport from the repository will be confined to a horizontally finite zone in the vicinity of the repository. Similar results have also been found in the present study. Therefore, we can conclude that the region around the repository will be a natural barrier for radionuclide containment. This type of modelling for the repository must be verified by additional numerical and analytical works, as well as a validation with laboratory and field experiments.

*Acknowledgement*—The authors appreciate the support from the Computer Center at Colorado State University and the U.S. Nuclear Regulatory Commission.

## REFERENCES

1. M. A. Combarnous and S. A. Bories, Hydrothermal convection in saturated porous media. In *Advances in Hydroscience*, Vol. 10, pp. 231–307 (1975).
2. I. Catton, Natural convection in enclosures, *Proc. 6th Int. Heat Transfer Conference*, Toronto, Vol. 6, pp. 209–235 (1979).
3. B. D. C. Chan, C. M. Ivey and J. M. Barry, Natural convection in enclosed porous media with rectangular boundaries, *J. Heat Transfer* **92,** 21–27 (1970).
4. C. G. Bankvall, Natural convection in vertical permeable space, *Wärme- und Stoffübertr.* **7,** 22–30 (1974).
5. J. E. Weber, The boundary layer regime for convection in a vertical porous layer, *Int. J. Heat Mass Transfer* **18,** 569–573 (1975).
6. P. J. Burns, L. C. Chow and C. L. Tien, Convection in a vertical slot filled with porous insulation, *Int. J. Heat Mass Transfer* **20,** 919–926 (1977).
7. K. L. Walker and G. M. Homsy, Convection in a porous cavity, *J. Fluid Mech.* **97,** 449–474 (1978).
8. P. G. Simpkins and P. A. Blythe, Convection in a porous layer, *Int. J. Heat Mass Transfer* **23,** 881–887 (1980).
9. C. E. Hickox and D. K. Gartling, A numerical study of

natural convection in a horizontal porous layer subjected to an end-to-end temperature difference, *J. Heat Transfer* **103**, 797–802 (1981).
10. A. Bejan, The boundary layer regime in a porous layer with uniform heat flux from the side, *Int. J. Heat Mass Transfer* **26**, 1339–1346 (1983).
11. V. Prasad and F. A. Kulacki, Natural convection in a rectangular porous cavity with constant heat flux on one vertical wall, *J. Heat Transfer* **106**, 152–157 (1984).
12. V. Prasad and F. A. Kulacki, Natural convection in a vertical porous annulus, *Int. J. Heat Mass Transfer* **27**, 207–219 (1984).
13. R. McKibbin and M. J. O'Sullivan, Onset of convection in a layered porous medium heated from below, *J. Fluid Mech.* **96**, 375–393 (1980).
14. R. McKibbin and M. J. O'Sullivan, Heat transfer in a layered porous medium heated from below, *J. Fluid Mech.* **111**, 141–173 (1981).
15. R. McKibbin and P. A. Tyvand, Anisotropic modelling of thermal convection in multilayered porous media, *J. Fluid Mech.* **118**, 315–339 (1982).
16. R. Rana, Numerical simulation of free convection in a multi-layer geothermal reservoir, M.S. Thesis, Department of Mechanical Engineering, University of Hawaii (1977).
17. R. Rana, R. N. Horne and P. Cheng, Natural convection in a multi-layered geothermal reservoir, *J. Heat Transfer* **101**, 411–416 (1979).
18. F. C. Lai and F. A. Kulacki, Natural convection in layered porous media partially heated from below, 24th ASME/AIChE National Heat Transfer Conference, Pittsburgh (1987).
19. D. Poulikakos and A. Bejan, Natural convection in vertically and horizontally layered porous media heated from the side, *Int. J. Heat Mass Transfer* **26**, 1805–1814 (1983).
20. S. V. Patankar, *Numerical Heat Transfer and Fluid Flow*. Hemisphere/McGraw-Hill, New York (1980).
21. A. Bejan and R. Anderson, Heat transfer across a vertical impermeable partition imbedded in porous medium, *Int. J. Heat Mass Transfer* **24**, 1237–1245 (1981).

## CONVECTION NATURELLE A TRAVERS UNE CAVITE POREUSE STRATIFIEE

**Résumé**—On étudie numériquement la convection naturelle permanente dans une cavité poreuse stratifiée bidimensionnelle chauffée sur un côté. On s'intéresse aux effets du rapport d'épaisseur de la sous-couche, du contraste de perméabilité et de la conductivité non uniforme dans un système comprenant deux couches. Les calculs couvrent un large domaine de ces paramètres. On observe que les champs de température et de vitesse avec $K_1/K_2 < 1$ sont complètement différents de ceux pour $K_1/K_2 > 1$. Quand les propriétés thermiques sont uniformes, le nombre de Nusselt moyen pour un système à $K_1/K_2 < 1$ est toujours supérieur à celui pour un système homogène et s'il augmente avec le nombre de Rayleigh, il décroît avec le rapport d'épaisseur de la sous-couche. Pour des systèmes à $K_1/K_2 > 1$, le nombre de Nusselt moyen est toujours moindre que pour le systeme homogène et il augmente à la fois avec le nombre de Rayleigh et le rapport d'épaisseur. Quand il existe une différence dans les conductivités des deux couches, une seconde cellule de recirculation est générée dans la couche la moins perméable pour $K_1/K_2 < 1$. Le nombre de Nusselt moyen augmente avec le rapport des conductivités pour $K_1/K_2 < 1$ et décroît pour $K_1/K_2 > 1$. On présente les résultats concernant les lignes de courant, les isothermes, les profils de température et de vitesse et le nombre de Nusselt en fonction du nombre de Rayleigh pour différentes valeurs des paramètres.

## NATÜRLICHE KONVEKTION IN EINEM SENKRECHTEN, MIT PORÖSEM MATERIAL GEFÜLLTEN HOHLRAUM

**Zusammenfassung**—Über numerische Untersuchungen der natürlichen Konvektion im stationären Zustand in einem zweidimensional geschichteten Hohlraum wird berichtet. Der Hohlraum ist mit porösem Material gefüllt und wird an einer Seitenwand beheizt. Insbesondere wurden die Einflüsse des Dickenverhältnisses der Unterschichten, des Unterschiedes in der Permeabilität und der inhomogenen Wärmeleitfähigkeit in einem System mit zwei Unterschichten untersucht. Die Berechnungen wurden über einen weiten Parameterbereich durchgeführt. Es wurde beobachtet, daß das Geschwindigkeits- und Temperaturfeld für eine geschichtete Struktur mit $K_1/K_2 < 1$ ganz anders sind als für $K_1/K_2 > 1$. Unter der Annahme einheitlicher Stoffwerte ist die mittlere Nusselt-Zahl in einem geschichteten System mit $K_1/K_2 < 1$ immer größer als in einem homogenen System, sie nimmt mit der Rayleigh-Zahl zu und mit dem Dickenverhältnis der Unterschichten ab. Bei Systemen mit $K_1/K_2 > 1$ ist die mittlere Nusselt-Zahl immer kleiner als im homogenen Fall und nimmt sowohl mit der Rayleigh-Zahl als auch mit dem Dickenverhältnis zu. Wenn die Wärmeleitfähigkeit in den beiden Unterschichten unterschiedlich ist, entsteht ein zweites Rückströmungsgebiet in der weniger durchlässigen Schicht, wenn $K_1/K_2 < 1$ ist. Die mittlere Nusselt-Zahl nimmt mit dem Verhältnis der Wärmeleitfähigkeit für $K_1/K_2 < 1$ zu und für $K_1/K_2 > 1$ ab. Die Wärmeübertragung wird dargestellt in Form von Stromlinien- und Isothermenbildern, Temperatur- und Geschwindigkeitsverteilungen und einer Beziehung der Nusselt-Zahl als Funktion der Rayleigh-Zahl für die genannten Parameter.

## ЕСТЕСТВЕННАЯ КОНВЕКЦИЯ В ВЕРТИКАЛЬНОЙ ПОЛОСТИ, ЗАПОЛНЕННОЙ СЛОИСТЫМ ПОРИСТЫМ МАТЕРИАЛОМ

**Аннотация**—Описаны численные исследования стационарной естественной конвекции в нагреваемой сбоку двумерной полости, заполненной слоистым пористым материалом. Цель исследования состояла в изучении влияния таких параметров, как отношение толщин двух подслоев, перепад проницаемостей и неоднородная теплопроводность в системе, состоящей из двух подслоев. Проведены расчеты в широком диапазоне этих параметров. Обнаружено, что поля течения и температуры для слоистой структуры с $K_1/K_2 < 1$ совершенно отличаются от соответствующих полей при $K_1/K_2 > 1$. При постоянных теплофизических характеристиках среднее значение числа Нуссельта для слоистой системы с $K_1/K_2 < 1$ всегда больше его среднего значения для однородной системы и увеличивается с ростом числа Рэлея, но уменьшается при увеличении отношения толщин подслоев. В системе с $K_1/K_2 > 1$ среднее значение числа Нуссельта всегда меньше его среднего значения для однородной системы и увеличивается с ростом как числа Рэлея, так и отношения толщин. При различной теплопроводности двух подслоев в слое с меньшей проницаемостью при $K_1/K_2 < 1$ образуется вторая ячейка с возвратной циркуляцией. Найдено, что с ростом отношения теплопроводностей среднее значение числа Нуссельта увеличивается при $K_1/K_2 < 1$ и уменьшается при $K_1/K_2 > 1$. Приведены картины линий тока и изотерм, профили температуры и скорости, а также зависимости числа Нуссельта от числа Рэлея и перечисленных выше параметров.